

Yale University

## EliScholar – A Digital Platform for Scholarly Publishing at Yale

---

Yale Medicine Thesis Digital Library

School of Medicine

---

January 2022

# Longitudinal Modeling Of Early Hiv Burden In The Central Nervous System

Victor Diego Armengol

Follow this and additional works at: <https://elischolar.library.yale.edu/ymtdl>

---

### Recommended Citation

Armengol, Victor Diego, "Longitudinal Modeling Of Early Hiv Burden In The Central Nervous System" (2022). *Yale Medicine Thesis Digital Library*. 4052.  
<https://elischolar.library.yale.edu/ymtdl/4052>

This Open Access Thesis is brought to you for free and open access by the School of Medicine at EliScholar – A Digital Platform for Scholarly Publishing at Yale. It has been accepted for inclusion in Yale Medicine Thesis Digital Library by an authorized administrator of EliScholar – A Digital Platform for Scholarly Publishing at Yale. For more information, please contact [elischolar@yale.edu](mailto:elischolar@yale.edu).

Longitudinal Modeling of Early HIV Burden in the Central Nervous System

A Thesis Submitted to the Yale University School of Medicine

in Partial Fulfillment of the Requirements for the Degree of Doctor of Medicine

by

Victor Diego Armengol

2022

## ABSTRACT

### LONGITUDINAL MODELING OF EARLY HIV BURDEN IN THE CENTRAL NERVOUS SYSTEM

V. Diego Armengol<sup>1</sup>, Veronika Shabanova<sup>2</sup>, Lars Hagberg<sup>3</sup>, Richard Price<sup>4</sup>, Magnus Gisslén<sup>3</sup>, Serena S. Spudich<sup>1</sup>.

<sup>1</sup> Department of Neurology, Yale University, School of Medicine, New Haven, CT.

<sup>2</sup> Department of Biostatistics, Yale University, School of Medicine, New Haven, CT.

<sup>3</sup> Gothenburg University, Gothenburg, Sweden.

<sup>4</sup> University of California San Francisco, San Francisco, CA.

**Background:** The dynamics of plasma HIV replication during early infection including establishment of a viral set-point are well-known. However, the course of HIV in the central nervous system (CNS) after initial entry of HIV into this compartment is less understood. Using longitudinal samples, we modeled the natural history of HIV RNA in the cerebrospinal fluid (CSF) and plasma during early HIV prior to initiation of antiretroviral treatment (ART).

**Methods:** Participants with primary HIV infection (PHI, within 12 months of initial infection) were enrolled in prospective studies with paired longitudinal sampling of blood and CSF conducted in San Francisco, USA, and Gothenburg, Sweden prior to test-and-

treat guidelines. This analysis incorporated all samples available over the first 3 years of infection from visits where participants were ART-naïve. HIV RNA assays had a lower limit of quantification of 40 copies per mL. Mean trajectory of CSF HIV RNA levels relative to time from infection was characterized using a restricted cubic spline function of time accounting for the correlated data within subjects. Parametric linear mixed effects models (LME) were also estimated to account for the covariate CD4/CD8 ratio and to confirm results from the spline analysis.

**Results:** The final analytical cohort included 110 PHI participants (95% male, median age = 37, days post infection = 91 at enrollment) with 228 CSF and 247 plasma measurements. The model shows an initial decrease in CSF HIV RNA over the first 100 days of estimated infection, after which CSF HIV RNA begins to increase at a slow rate. Similar trends were seen in the plasma model, but at higher absolute values of HIV RNA copies/mL and with a narrower confidence interval compared to CSF. Plasma-CSF viral load difference declined rapidly in the first 100 days of infection. We confirmed the mean trajectory of change in HIV RNA derived from the cubic splines approach using the parametric LME model. Blood CD4/CD8 ratio negatively correlated with CSF HIV RNA, as there was a 0.69 unit decrease in  $\log_{10}(\text{CSF HIV RNA})$  for each unit increase in the CD4/CD8 ratio ( $p = 0.0005$ ).

**Conclusions:** The viral dynamics in the CSF of ART-naïve individuals over the first 36 months of infection support the early spread of HIV to the CNS, and indicate that HIV replication is maintained in this compartment throughout the course of early infection

prior to ART. Early initiation of ART may limit nervous system exposure to pathogenic effects of viral replication.

## ACKNOWLEDGEMENTS

Firstly, I would like to thank everyone who participated in this study.

Thank you to my thesis advisor and research mentor, Dr. Serena Spudich, without whom this thesis would not have been possible. I am also grateful to Drs. Richard Price, Lars Hagberg, and Magnus Gisslén for their work identifying participants and collecting samples, along with the research coordinators, laboratory investigators, and staff who facilitated sample processing and generated the data analyzed in this project. I would also like to thank Dr. Veronika Shabanova for her expertise and contributions, and for patiently helping me learn new concepts.

Thank you to my fiancée, Steph, for her encouragement throughout this journey.

Finally, I am grateful for my parents, Humberto and Susana, whose unwavering support and love has meant the world to me.

The research included in this thesis was supported by the National Heart, Lung and Blood Institute of the National Institutes of Health under Award Number T35HL007649. The studies through which the specimens and laboratory, clinical and demographic data were collected were supported by the National Institutes of Health (grants R01 MH081772, K23 MH074466) and the Sahlgrenska Academy at the University of Gothenburg (grant ALFGBG-430271).

## TABLE OF CONTENTS

Introduction.....	1
Statement of purpose.....	10
Methods.....	12
Results.....	17
Discussion.....	27
References.....	34

## INTRODUCTION

Human immunodeficiency virus (HIV) is a retrovirus which has affected over 75 million people worldwide since the start of the epidemic in the 1980s [1]. The arrival of this epidemic was first noted as a state of severe immunodeficiency – now called acquired immune deficiency syndrome (AIDS) – but discovery of HIV itself would follow within 2 years of the first report of AIDS [2-4]. In the decades since its discovery, an immense amount of research has gone into learning how the virus propagates, strategies for preventing HIV transmission, and pharmacological treatment for people living with HIV.

In 2015, the findings of the Strategic Timing of Antiretroviral Therapy (START) trial were published. This randomized controlled trial showed better outcomes for HIV-positive adults who initiated antiretroviral therapy (ART) at CD4+ T cell counts of over 500 cells per mm<sup>3</sup> compared to those who initiated ART only once their CD4+ T cell count decreased below 350 cells per mm<sup>3</sup> [5]. In response to the START trial, the World Health Organization (WHO) announced new guidelines, called ‘treat-all’ (now known as ‘test-and-treat’). This change expanded treatment eligibility from 28 million people to all 37 million people estimated to be living with HIV at the time [6].

Given the extent of research into HIV, and especially from *in vivo* models of the related simian immunodeficiency virus (SIV) in macaques, the progression of HIV infection can be described in detail. Infection with HIV usually occurs when the virus crosses a mucosal barrier and infects its main target, CD4+ T cells. Following this event, the host CD4+ T cells produce more copies of the virus, and these virions then spread to

the lymphatic system. It is in the lymphoid tissue (accessed via the bloodstream from the initial draining lymph nodes) where HIV infection truly takes hold due to the presence of greater quantities of CD4<sup>+</sup> T cells, thus resulting in true self-propagation as the virus'  $R_0$  exceeds 1. Migration to the gut-associated lymphoid tissue in particular causes profound depletion of CD4<sup>+</sup> T cells [7]. The presence of HIV-infected resting CD4<sup>+</sup> T cells is thought to be one reason that effective ART cannot fully 'cure' HIV within the human lifespan, as these cells have half-lives exceeding 40 months [8].

Bloodborne HIV can be detected by about day 10 of infection. Exponential replication of the virus soon follows over a period of weeks, reaching a peak of about  $10^6 - 10^7$  copies per mL of plasma, coinciding with an acute symptomatic period of flu-like illness and lymphadenopathy in some individuals. This peak in plasma viral RNA is followed by a precipitous decline and, in most individuals, the amount of virus in the plasma reaches a low plateau, termed the 'viral set point' [9]. It generally takes 4-6 months to reach this set point, at which point the acute/primary phase of infection concludes [1].

Coinciding with the decrease of plasma viral load following its early peak is the depletion of blood CD4<sup>+</sup> T cells, which reach a nadir at around 6 weeks post-infection. Afterward, the CD4<sup>+</sup> T cell count usually recovers to near-normal levels by about 12 weeks, by which point the viral load has reached its set point. However, over the subsequent years, untreated HIV slowly depletes the body's CD4<sup>+</sup> T cells by creating a state of constant activation – and subsequent death – of both CD4<sup>+</sup> and CD8<sup>+</sup> T cells [1]. Research has shown this T cell activation to be an independent predictor of the rate of

CD4<sup>+</sup> T cell decline and AIDS progression [10, 11]. Following the trajectory of the CD4<sup>+</sup> T cell count over time has been important for clinical care, as severe infections become more common with counts under 350 cells per  $\mu\text{L}$ ; one of the criteria for a diagnosis of AIDS is a CD4<sup>+</sup> T cell count of less than 200 cells per  $\mu\text{L}$ . **Figure 1** summarizes these changes in plasma viral load and blood CD4<sup>+</sup> T cell count over time [1, 12].

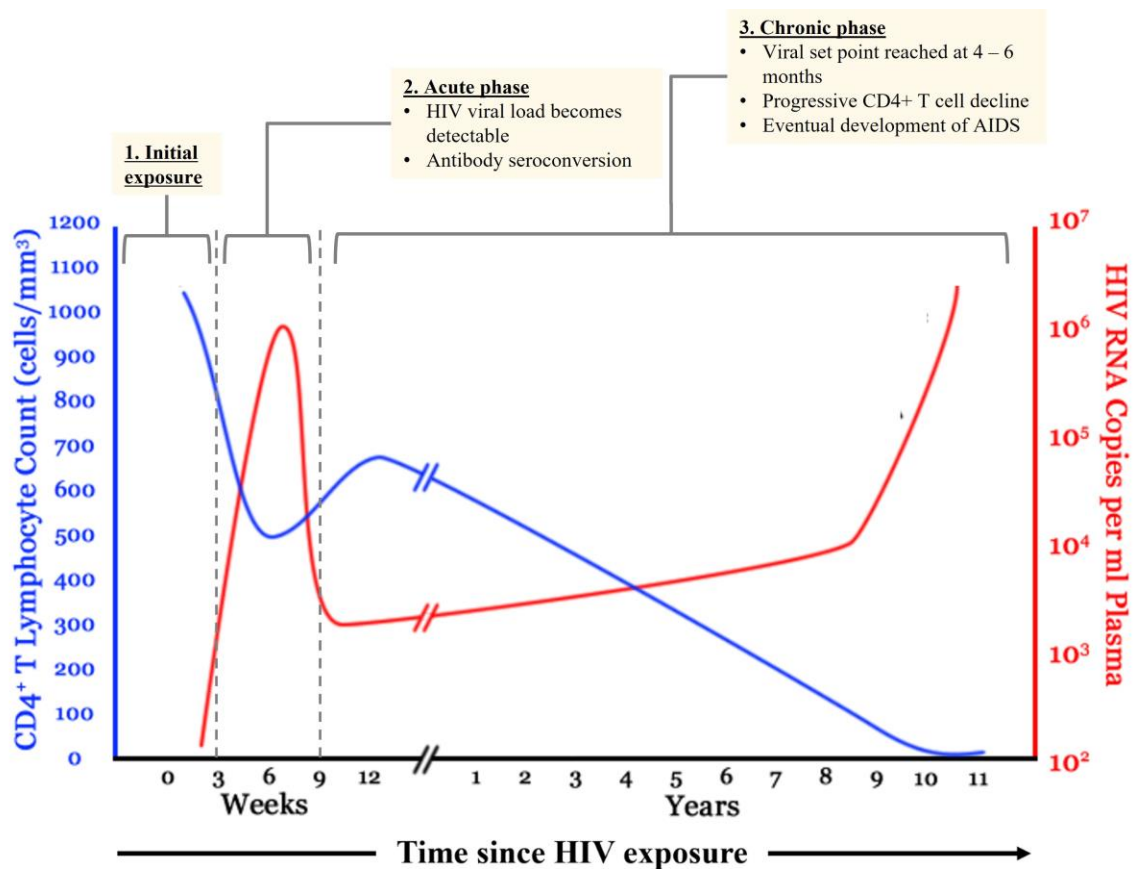


**Figure 1.** Schematic representation of plasma viral load (red) and blood CD4<sup>+</sup> T cell count (blue) during the natural course of HIV infection. Adapted from Giorgi, 2011 and Deeks et al., 2015.

Importantly, there is individual variation in the absolute value of the peak viral load and viral set point, which can fall between a wide possible range. A greater quantity of symptoms during primary infection has been found to be predictive of higher initial viral loads, and severity of symptoms shows a similarly positive correlation. A greater quantity of infectious symptoms is also associated with a higher viral set point [13]. Moreover, higher viral set points have long been known to be predictors of a poor prognosis, and viral load is actually a more reliable predictor of progression to AIDS than CD4+ T cell count, despite the widespread use of the latter measure in the clinical setting [14].

Some individuals with HIV, termed ‘elite controllers’, naturally exhibit viral set points below the limit of detection of typical assays, which usually corresponds to fewer than 50 copies of HIV RNA per mL plasma. One of the leading theories attempting to explain this phenomenon centers around CD8+ T cells, as these cells have been shown to inhibit viral replication during primary infection. This likely does not fully explain the phenomenon, as some elite controllers lack an HIV-specific CD8+ T cell response, thus more investigation will be needed to better understand the mechanisms behind elite controllers’ natural viral suppression [15, 16].

HIV has long been known to affect the central nervous system (CNS) [17], with documented effects including cognitive impairment, inflammation, neuronal damage, and cortical thinning [18-22]. Additionally, preferential loss of volume in the putamen has been seen in individuals with early HIV infection [23]. The range of neurological symptoms seen in individuals living with HIV, termed HIV-associated neurocognitive

disorder (HAND), includes asymptomatic neurocognitive impairment, mild neurocognitive disorder, and HIV-associated dementia (HAD) in the most severe cases. While ART is the only known way to impede the progression of HAND, these symptoms can still occur in individuals who are receiving treatment [24]. In a study of macaques with SIV, ART was found to prevent the development of SIV encephalitis when compared to infected macaques that did not receive treatment, and even resulted in the absence of virus in postmortem brain samples of treated macaques, despite the use of ART drugs that could not cross the blood-brain barrier (BBB) [25].

Moreover, HIV is a neurotropic virus which leads to infection of cells within the CNS, and the neuropathogenesis of this process is an area of active investigation. The process is thought to begin with inflammation and breakdown of the BBB, with one study finding that some individuals are susceptible to severe disruption of the BBB persisting beyond 1000 days after infection (as measured by elevations in the cerebrospinal fluid [CSF] to serum albumin quotient), and that this phenomenon is associated with changes in CSF biomarkers indicative of greater CNS involvement. The authors also noted that initiation of ART (at a median of 225 days after infection) successfully suppressed viral replication in both CSF and plasma, as well as reduced signs of CNS inflammation, but did not change BBB permeability [26]. While systemic inflammation is likely responsible for the initial sequence of events resulting in HIV translocation across the BBB and neurodegeneration, other mechanisms are suspected to contribute to the development of HAND, such as changes to the release and uptake of glutamate. Specifically, the HIV proteins tat and envelope glycoprotein gp120 can stimulate glutamate release and decrease its synaptic uptake, which, along with phosphorylation of glutamate receptors

and incomplete glutamate recycling via the glutamate-glutamine shuttle, contributes to augmented glutamate toxicity [24].

Despite the reduction in CSF viral load often seen after the initiation of ART, other studies have shown that HIV is capable of establishing a viral ‘reservoir’ in the CSF that, in some individuals, can persist even in those receiving long-term ART [27, 28]. This phenomenon, termed ‘CSF escape’, has been associated with worsening neurologic function and thus is implicated in the development of HAND [29-32].

When CSF escape occurs, it is posited to be caused by HIV remaining in CNS microglia, resulting in reseeding of other tissues and contributing to ART resistance; accordingly, these cells have become a focus of intense research [33]. While HIV has also been detected in astrocytes in some studies, whether they can be considered cellular reservoirs of the virus remains controversial [34, 35]. Regardless, the presence of viral reservoirs such as that seen in the CNS impede eradication of the virus and thus prevent a true cure.

As previously discussed, the dynamics of HIV replication in the blood plasma during acute infection are well-known [36]. Similar dynamics of HIV infection have been studied in other tissues of the body, which creates viral compartments. This process has been documented in the CNS and genital tract, but also likely occurs in the gut, lung, liver, kidney, and breast milk [37].

One example is the semen, where HIV viral load was found to have an early peak, similar to that seen in plasma, in one prospective cohort study of men with acute HIV

infection in Lilongwe, Malawi. This was followed by a stable, suppressed level. However, the viral load in plasma peaked earlier than that of the semen (~17 days post-infection compared to ~30 days in semen) [38]. The absolute values of both the estimated peak and viral set point in the semen were found to be lower than those in the plasma [39].

Studies of HIV in the CNS rely primarily on brain tissue at autopsy or on CSF analysis. These have led, for example, to the discovery that the virus in the brains of people with HIV-associated dementia is genetically distinct from the virus in those without HIV-associated dementia [40]. However, in order to study HIV in the CNS of living people, CSF must be analyzed. Studies using CSF have led to similar discoveries showing that viral populations in the CSF and plasma are genetically distinct from one another [41, 42].

Prior studies, such as those involving the RV254/SEARCH010 cohort, a large cohort of mostly male participants in Bangkok, Thailand identified during acute HIV infection, have investigated the neuropathogenesis of HIV. In one such prospective study, investigators noted that HIV RNA could be detected in the CSF of participants as early as 8 days after infection with the virus. Inflammation of the CNS was noted in some participants, whose CSF showed elevations in inflammatory markers such as neopterin, monocyte chemoattractant protein-1/CCL2, and interferon  $\gamma$ -induced protein 10/CXCL-10 levels. Signs of brain parenchymal inflammation were also noted on magnetic resonance spectroscopy (MRS) – specifically, higher choline/creatine in the occipital gray matter at the middle posterior cingulate gyrus – when these participants were compared to

individuals living with chronic HIV as well as HIV-negative Thai controls. They also noted that headache, while a common symptom in the acute phase of infection, was not accompanied by any other acute neurological signs or symptoms [43].

In contrast, a different observational study combining cohorts of participants with primary HIV infection – including the Primary Infection Stage CNS Events Study (PISCES) cohort in San Francisco, USA as well as cohorts in Gothenburg, Sweden, Milan, Italy, and Sydney, Australia – found that some neurological symptoms do develop during primary infection, such as encephalitis, clinical meningitis, lower motor neuron facial palsy, distal paresthesia, photophobia with intense headache, acute painful polyradiculopathy, and brachial neuritis [44]. Another study, also involving the PISCES cohort, found that major depressive disorder was prevalent among participants during primary infection, with greater somatic symptoms than cognitive/affective symptoms and decreased vigor scores relative to controls, and that these findings did not change over longitudinal follow-up prior to initiation of ART [45].

Notably, viral compartmentalization is not a phenomenon solely seen with HIV. Examples in the literature include the lifelong persistence of BK virus in kidney tubule epithelial cells and urinary tract epithelial cells [46], the presence of hepatitis C virus in extrahepatic tissue such as the B cells and macrophages of the colon [47] as well as platelets [48], and the establishment of reservoirs of human papillomavirus in the hair follicle stem cells of healthy individuals [49].

The JC virus has even been shown to undergo a dynamic reorganization process that is compartment-specific: in individuals with progressive multifocal

leukoencephalopathy (PML), the viral population in the CSF is composed of a mixture of viral variants that is correlated to that seen in plasma, but significantly different from the population in urine, which mostly consists of the archetypal JC virus strain [50]. In a case report of an immunocompromised person who died from PML, autopsy showed distinct viral rearrangements in different regions of the brain, suggesting multiple independent origins for the lesions [51].

In comparison to plasma, the natural progression of HIV penetration into the CSF is less understood. Despite our knowledge of CSF escape, important questions remain regarding at which point during the course of infection this viral reservoir is established, prior to initiation of ART. A detailed analysis of this process would be an important further step in continuing to understand the natural course of HIV and its establishment of a CNS reservoir. We undertook a prospective longitudinal study of early infection in treatment-naïve participants and characterized the trajectory of change of HIV viral load in the CSF.

## STATEMENT OF PURPOSE

We aimed to create a mathematical model to describe the natural dynamics of HIV in the CSF during early infection. To do so, we used data from a prospective longitudinal observational study of individuals identified during early infection and conducted an analysis using a subset of treatment-naïve participants. Once a model for CSF HIV burden during early infection was created, we compared it to the dynamics in plasma. We expected that the peak viral load would be lower than that found in the plasma and would occur later during the course of infection. However, we anticipated that the initial peak may not be fully determinable based on the timing of baseline visits in the cohort. We also expected the viral set point for CSF HIV burden to be established early in the course of infection and to remain stable over time, as is seen in the plasma model. Moreover, we created models for the plasma-CSF viral load difference and the blood CD4/CD8 T cell ratio over the same period of time. The plasma-CSF viral load difference was expected to remain positive as viral load is generally higher in the plasma relative to CSF. The CD4/CD8 ratio was expected to decrease as plasma viral load increases, and we predicted the same relationship would be true with CSF viral load.

### *Specific Aims*

1. Create a nonparametric model for CSF HIV RNA dynamics using longitudinal data.

- a. Model plasma HIV burden using the same longitudinal data and compare the dynamics of HIV distribution in these two compartments.
  - b. Model the logarithmic difference between plasma and CSF viral loads using the same longitudinal data.
  - c. Model the blood CD4/CD8 ratio using the same longitudinal data and describe trends.
2. Create a parametrized model to approximate the nonparametric model from Specific Aim 1.
- a. Use the nonparametric model to estimate potential knots in parametrized model.
  - b. Determine whether potential covariates such as CD4/CD8 ratio and polynomials of time since infection are significantly associated with CSF viral load.

## METHODS

### *Student Contributions*

All data analysis (described below) and generation of figures was conducted by the author (V. Diego Armengol) with guidance from Veronika Shabanova, PhD and Serena Spudich, MD, MA. This included application of exclusion criteria to the overall set of data to select an appropriate set of data from cohorts of ART-naïve participants, as well as the generation of both the nonparametric longitudinal models and the parametrized models. This analysis uses pre-existing data from larger observational studies conducted in San Francisco, USA by Serena Spudich, MD, MA and Richard Price, MD, and in Gothenburg, Sweden by Lars Hagberg, MD, PhD and Magnus Gisslén, MD, PhD.

### *Ethics Statement*

Participation in the longitudinal observational studies which produced the data used in this analysis (described below) was entirely voluntary and all participants gave written informed consent. Participants who were identified during primary HIV infection were enrolled in prospective studies and returned for as many repeat blood draws, lumbar punctures, neuroimaging, and cognitive studies as they wished. Participants were also at liberty to consent to some measurements but not others at each encounter (e.g., during a given study visit they could consent to a blood draw but not a lumbar puncture).

Moreover, the collection of this data had no bearing on their individual medical treatment for HIV or otherwise.

As data collection occurred prior to the application of universal test-and-treat guidelines, it is important to note that participation in this study had no influence on the date of ART initiation. This resulted in a unique subset of observational data from participants who remained ART-naïve, which can no longer be recreated in the age of test-and-treat.

### *Participants and Data Collection*

This is a secondary analysis of data from the PISCES cohort in San Francisco, USA, and a complementary study of individuals with primary HIV infection in Gothenburg, Sweden, which have been previously described [26, 44, 52]. Briefly, participants were originally enrolled in neurological early HIV infection studies between November 1986 and February 2014 at 2 institutions: the University of California, San Francisco and the University of Gothenburg in Sweden. All potential participants were screened for primary HIV-1 infection with the Serological Testing Algorithm for Recent HIV Seroconversion (STARHS) [53, 54].

Individuals with early infection – as demonstrated by a recent positive HIV-1 nucleic acid test, and a negative test in the prior 12 months, or less commonly an antibody test indicating recent infection – were invited to participate. Participants with an enzyme immunoassay result indicating infection within the past 6 months were also

offered enrollment. All participants were ART-naïve at enrollment. An approximate date of infection for each participant was estimated according to standard clinical and laboratory parameters (date of HIV transmission from donor to host was estimated as 14 days prior to the onset of any symptoms of an acute retroviral syndromes, or as the halfway point between the last negative and first positive test) [55]. Participants in the PISCES cohort were presumed to be infected with clade B viruses, whereas HIV subtype information was collected for some participants in the Gothenburg cohort given their more diverse geographic origin [44].

Study visits were scheduled at baseline, 6 weeks, and every 6 months thereafter, although there was participant variation in the timing and duration of follow-up. CSF and blood specimens were obtained and processed at each visit as previously described [19, 45, 56, 57]. HIV RNA was measured in both the CSF supernatant (cell-free fraction of CSF) and blood plasma using the Roche Amplicor Monitor assay at both sites, with a quantitation limit of 50 copies/mL and a detection limit of 20 copies/mL [52, 58].

Viral load results for both CSF and plasma were calculated as  $\log_{10}(\text{HIV RNA copies/mL})$ . Detectable results less than 50 copies/mL were reported with a value of 1.69 (equivalent to  $\log_{10} 49$ ). Additionally, a plasma-CSF viral load difference was calculated, which is equivalent to  $\log_{10}(\text{HIV RNA copies per mL CSF}) - \log_{10}(\text{HIV RNA copies per mL plasma})$ . Analysis of CSF and flow cytometry for blood CD4+ and CD8+ T lymphocyte counts were performed as previously described, along with testing for other biomarkers not applicable to the current analysis [52].

### *Statistical analysis*

Continuous variables were summarized using means with standard deviations or medians with Intra Quartile Range (IQR: 25<sup>th</sup> percentile, 75<sup>th</sup> percentile), while categorical variables were summarized with frequencies and percentages. The mean trajectory of CSF HIV RNA levels relative to time from initial HIV transmission was characterized using a restricted cubic spline function of the time variable accounting for the correlated data within subjects, with the fit of the model bootstrapped 1000 times, treating a subject as a cluster [59-63]. The simultaneous 95% confidence region for the entire regression curve was also estimated accounting for the subject clusters and plotted relative to time since infection [64].

Data analysis was conducted using R [65] and function `rm.boot` in the package `Hmisc` [66]. Parametric linear mixed effects (LME) models with a knot at 100 days and time effect up to the third-degree polynomial before and after the knot were also estimated to account for the covariate CD4/CD8 ratio and to confirm the results from the spline analysis. Nested models for the different polynomial degrees of time were compared using the likelihood ratio test (LRT).

We chose among a random intercept model for the covariance and an additional random slope effect using the LRT with a mixture chi-square distribution. The estimation of parameters in the LMEs and the splines was implemented using the full or restricted maximum likelihood approach, which made it possible to keep all subjects in the model by treating the missing outcome values as missing at random (MAR) [67]. The same approach was used to characterize plasma HIV RNA levels, the plasma-CSF HIV RNA

level difference, and blood CD4/CD8 ratio. The R package nlme [68] was used to fit the LMEs.

To quantify the variability among CSF viral load measurements, we calculated and plotted a semivariogram for possible pairs of time points. In the model for the mean of the outcome we used variables for time since infection (linear and quadratic), time after 100 days of infection (linear, quadratic and cubic), and CD4/CD8 ratio. The plot revealed proportionate contributions from a possible measurement error, serial within-person correlation in time, and between-person variability, i.e., variance of random effect(s). Once it was revealed that the majority of variability in the outcome was due to the subject-specific characteristics, an Intra Class Correlation (ICC) was estimated to quantify the variability among subjects in the HIV RNA CSF levels as a ratio of the variance of the random intercept to the total variance. All statistical hypotheses tests were conducted at the two-sided alpha level of 0.05.

## RESULTS

### *Study participant characteristics*

The original San Francisco PISCES cohort included 109 participants, while the Gothenburg primary infection CNS study included 27 participants, for a total of 136 participants. Among these participants over time, 491 total CSF specimens and CSF HIV viral load measurements were collected. After excluding all study visits in which participants had already begun ART, 130 participants and 246 CSF measurements remained eligible for the analysis (**Figure 2**). In order to minimize the undue influence of some observations on the statistical models, we excluded visits after 3 years post-infection, followed by manual exclusion of some CSF measurements from one participant (who had 13 total CSF measurements over 2 years) to ensure a maximum of 7 CSF measurements per participant. Following application of these exclusion criteria, we then excluded all remaining participants who no longer had applicable CSF measurements (i.e., participants who had plasma measurements without paired CSF measurements prior to ART initiation). The final analytical cohort included 110 subjects, with 228 CSF measurements and 247 plasma measurements. Participants overall had an average of 2.3 visits (median = 2) to contribute to the analysis.

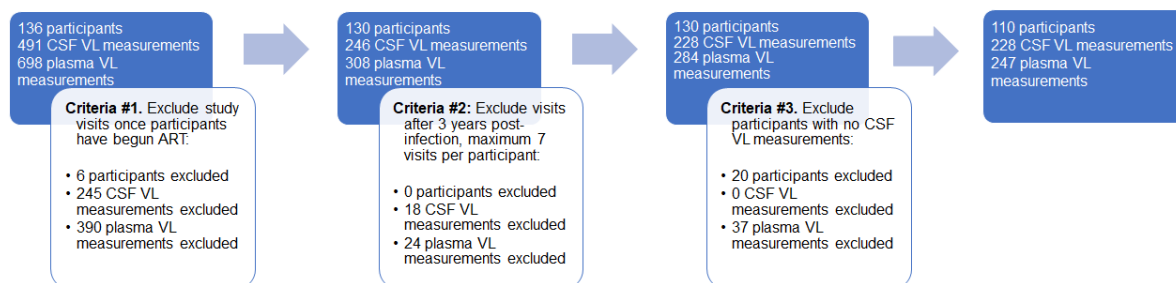


**Figure 2. Description of sequential exclusion criteria applied to initial cohort of participants. After excluding all study visits after the initiation of ART, excluding visits after 3 years post-infection, ensuring a maximum of 7 CSF measurements per participant, and excluding all remaining participants without applicable CSF measurements after application of prior exclusion criteria, the final cohort contained 110 participants, 228 CSF viral load measurements, and 247 plasma viral load measurements. VL = viral load.**

**Table 1** shows the demographic characteristics of the participants included in this analysis. Overall, the population was 95% male and 5% female. Despite the sex imbalance, the female participants were retained because on empirical analysis, their CSF viral burden over time was not systematically different from that of the male participants, and a different physiologic response is not expected based on sex. Data on race and

ethnicity was only collected at the San Francisco site; for that group of participants (n=83), 71% were Caucasian, 11% were Black, and 8% were Asian, with 20% identifying as Hispanic/Latino. HIV subtype was only determined at the Gothenburg site; while subtype was not explicitly confirmed at the San Francisco site, all participants there were presumed to have the HIV-B subtype.

	Site 1 (n = 83)		Site 2 (n = 27)		Total (n = 110)	
	n	%	n	%	n	%
<b>Gender</b>						
Male	83	100	22	81.48	105	95.45
Female	0	0	5	18.52	5	4.55
N/A	0	0	0	0	0	0
<b>Race</b>						
Caucasian	59	71.08	0	0	59	53.64
African-American/Black	9	10.84	0	0	9	8.18
Asian	7	8.43	0	0	7	6.36
American Indian/Alaska Native	1	1.20	0	0	1	0.91
Native Hawaiian/Pacific Islander	1	1.20	0	0	1	0.91
More than one race	3	3.61	0	0	3	2.73
Other, unknown or not reported	3	3.61	0	0	3	2.73
N/A	0	0	27	100	27	24.55
<b>Ethnicity</b>						
Hispanic/Latino	17	20.48	0	0	17	15.45
Non Hispanic/Latino	66	79.52	0	0	66	60
N/A	0	0	27	100	27	24.55
<b>HIV Subtype</b>						
A	0	0	1	3.70	1	0.91
A/D	0	0	1	3.70	1	0.91
B	0	0	9	33.33	9	8.18
C	0	0	4	14.81	4	3.64
CRF01_AE	0	0	2	7.41	2	1.82
CRF02_AG	0	0	2	7.41	2	1.82
CRF02_AG/G	0	0	1	3.70	1	0.91
N/A	83	100	7	25.93	90	81.82
<b>Education (years)</b>						
	Mean (SD)		Mean (SD)		Mean (SD)	
	15.02 (2.48)		N/A		15.02 (2.48)	
<b>Age at first visit (years)</b>						
	35.48 (9.16)		43.52 (13.04)		37.45 (10.76)	

**Table 1. Demographic characteristics of cohort, separated by site. Site 1 = University of California, San Francisco, USA; Site 2 = University of Gothenburg, Sweden; SD = standard deviation.**

*Individual CSF viral load trajectories*

On average, participants' CSF viral loads were followed for 295 days post-infection (median = 152, minimum = 14, maximum = 1087) and their plasma viral loads were followed for an average of 320 days post-infection (median = 182, minimum = 14, maximum = 1087). Participants had a mean of 2.07 CSF measurements and 2.25 plasma measurements taken each (median = 2, minimum = 1, maximum = 7 for both CSF and plasma). In total, there were 226 instances where treatment-naïve participants had both CSF and plasma HIV RNA levels measured.

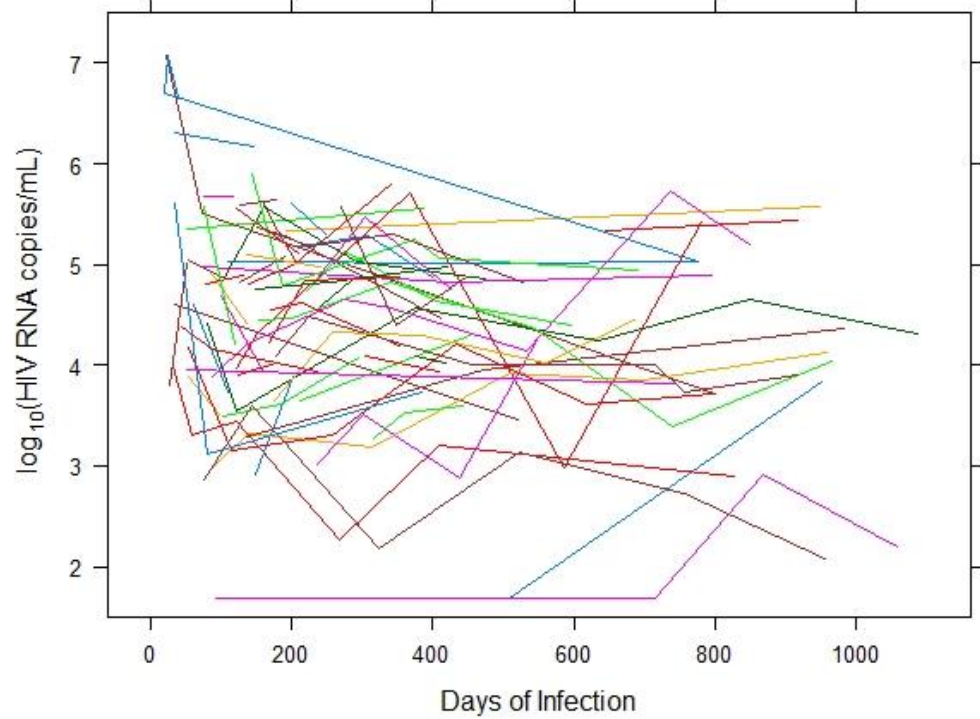
As shown in **Table 2**, a slight majority of the CSF viral load measurements (115 of 228, or 50.4%) were obtained during the first 6 months of infection. However, a notable proportion of CSF viral load measurements were obtained between 1-3 years post-infection (60 of 228, or 26.3%), supporting the longitudinal nature of this analysis. Similar trends were also true of measurements of plasma viral load (119 of 247, or 48.2% of measurements during the first 6 months; 73 of 247, or 30.0% of measurements between 1-3 years post-infection) and of CD4/CD8 ratios (117 of 249, or 47.0% of measurements during the first 6 months; 76 of 249, or 30.5% of measurements between 1-3 years post-infection).

Months Since Infection (,]	Median log <sub>10</sub> [HIV-1 RNA CSF Viral Load] (IQR)		Median log <sub>10</sub> [HIV-1 RNA Plasma Viral Load] (IQR)		Median Plasma - CSF VL Difference		Median CD4/CD8 Ratio (IQR)	
	N		N		N		N	
0-2	38	3.10 (2.55 - 3.89)	37	4.90 (4.24 - 5.79)	37	1.86 (1.47 - 2.29)	35	0.50 (0.33 - 0.78)
2-4	42	2.59 (1.69 - 3.32)	43	4.60 (3.90 - 5.05)	41	1.87 (1.37 - 2.34)	43	0.66 (0.44 - 0.77)
4-6	35	2.73 (1.69 - 3.43)	39	4.43 (3.93 - 5.21)	35	1.75 (1.32 - 2.21)	39	0.69 (0.44 - 0.91)
6-8	25	3.11 (2.47 - 3.98)	25	4.84 (4.46 - 5.18)	25	1.42 (1.05 - 1.92)	25	0.53 (0.39 - 0.80)
8-10	13	2.69 (2.20 - 3.77)	14	4.85 (4.14 - 5.02)	13	1.81 (0.91 - 2.13)	15	0.72 (0.49 - 1.01)
10-12	15	3.07 (1.98 - 3.54)	16	4.38 (3.52 - 4.98)	15	1.72 (1.56 - 1.81)	16	0.42 (0.34 - 0.76)
12-14	15	3.24 (2.49 - 3.49)	18	4.70 (4.14 - 5.04)	15	1.39 (1.28 - 1.70)	19	0.46 (0.29 - 0.53)
14-16	10	2.69 (2.14 - 3.56)	10	4.11 (3.68 - 4.72)	10	1.15 (0.48 - 1.42)	10	0.81 (0.57 - 1.04)
16-18	5	2.54 (2.37 - 2.71)	7	3.92 (3.30 - 4.25)	5	1.03 (0.43 - 1.08)	7	0.55 (0.44 - 0.66)
18-20	3	1.81 (1.75 - 2.91)	4	4.13 (3.76 - 4.28)	3	2.33 (1.36 - 2.38)	5	0.53 (0.36 - 1.27)
20-22	3	2.83 (2.46 - 3.24)	3	4.24 (3.93 - 4.79)	3	1.52 (1.47 - 1.61)	4	0.63 (0.54 - 0.71)
22-24	4	2.79 (2.27 - 3.52)	6	4.06 (3.89 - 4.37)	4	0.91 (-0.15 - 1.86)	6	0.55 (0.35 - 1.03)
24-26	6	3.39 (3.26 - 3.96)	8	3.78 (3.49 - 5.12)	6	0.49 (0.29 - 0.79)	8	0.47 (0.38 - 0.57)
26-28	6	3.33 (2.51 - 3.80)	6	4.19 (3.72 - 4.83)	6	1.27 (0.73 - 1.41)	6	0.55 (0.53 - 0.73)
28-30	1	1.69 (1.69 - 1.69)	1	2.91 (2.91 - 2.91)	1	1.22 (1.22 - 1.22)	1	1.21 (1.21 - 1.21)
30-32	4	2.49 (2.13 - 2.93)	7	4.03 (3.86 - 4.78)	4	1.99 (1.72 - 2.40)	7	0.44 (0.33 - 0.47)
32-34	1	4.20 (4.20 - 4.20)	1	4.37 (4.37 - 4.37)	1	0.17 (0.17 - 0.17)	1	1.02 (1.02 - 1.02)
34-36	2	2.35 (2.02 - 2.69)	2	3.26 (2.73 - 3.79)	2	0.90 (0.71 - 1.10)	2	0.79 (0.57 - 1.02)
Total	228	-	247	-	226	-	249	-

**Table 2. Summary of median CSF and plasma viral loads, their difference, and CD4/CD8 ratio for the first 3 years after seroconversion, grouped into 2-month intervals. IQR = interquartile range.**

Individual trajectories of CSF viral load measurements varied greatly among participants, as quantified by an ICC=0.6589. When looking at individual trajectories, CSF viral load appeared to initially decrease, often below the limit of detection, before eventually rising, sometimes hundreds of days post-infection (**Figure 3**). As seen in **Figure 4**, the total variance of log<sub>10</sub>(CSF HIV RNA) is about 0.74, which is composed of a small measurement error. The lack of a steady increase in the semivariogram suggested no decay in within-person correlation as time between data points increases, and between-person variability was likely the largest contributor of variability.

**(a) Plasma Viral Load, Individual Participants**



**(b) CSF Viral Load, Individual Participants**

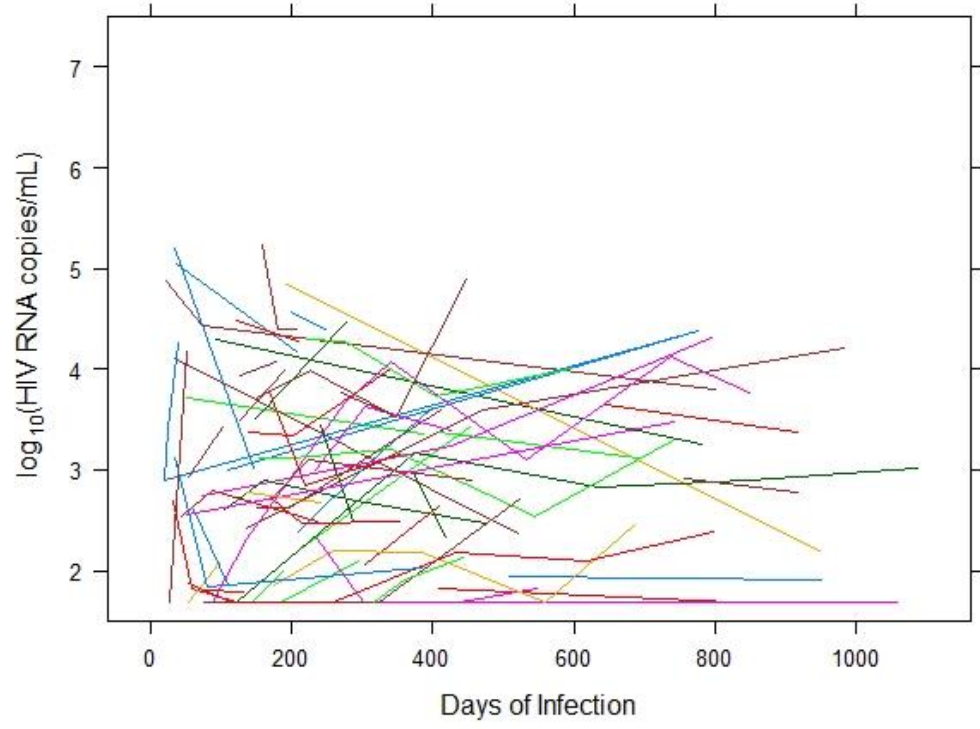


**Figure 3. Trajectories of (a) plasma HIV viral loads and (b) CSF HIV viral loads of individual participants over time when longitudinally sampled, prior to initiation of antiretroviral therapy.**

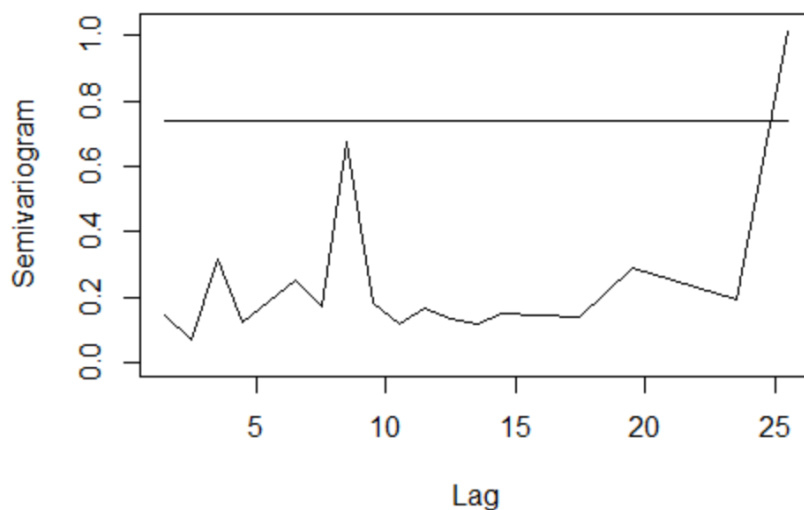


**Figure 4. Semivariogram quantifying variability among CSF viral load measurements. The x-axis represents time (in months) since infection.**

#### *Longitudinal models*

The longitudinal mean trajectory of HIV viral load in the CSF using the cubic splines approach is plotted in **Figure 5** along with the 95% confidence interval. The model shows an initial decrease in CSF viral load over the first 100 days of infection, after which viral load begins to increase at a slow rate. The 100-day mark was noted to be an inflection point in the model, which later guided our choice of a knot in the parametric LME model. Similar trends were seen in the plasma viral load model, but at higher

absolute values of HIV RNA copies/mL and with a narrower confidence interval when compared to the CSF, especially during the early post-infection period. Accordingly, our model of the plasma-CSF viral load difference showed a rapid decline in the first 100 days of infection, reflecting the initial higher magnitude of plasma viral load when compared to the peak of CSF viral load. Toward the end of the 3-year period described by the model, this difference begins to increase, driven by the increase in plasma viral load seen over the same time period. Finally, our model of blood CD4/CD8 ratio showed an initial trough at around 100 days, followed by a peak around 200 days, and a steady decline thereafter. **Figure 6** shows these same longitudinal models with individual data points superimposed.

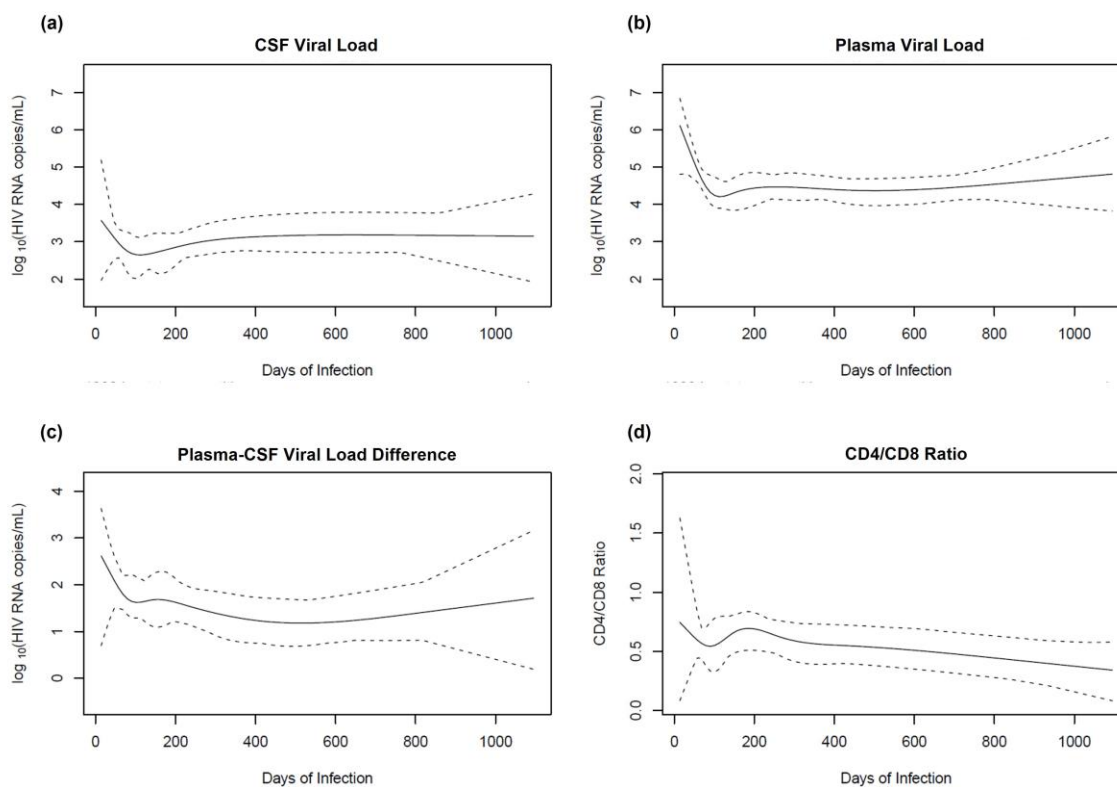


**Figure 5. Nonparametric models of (a) CSF HIV viral load, (b) plasma HIV viral load, (c) the difference in viral load between plasma and CSF, and (d) blood CD4/CD8 ratio over time in participants prior to antiretroviral therapy.**

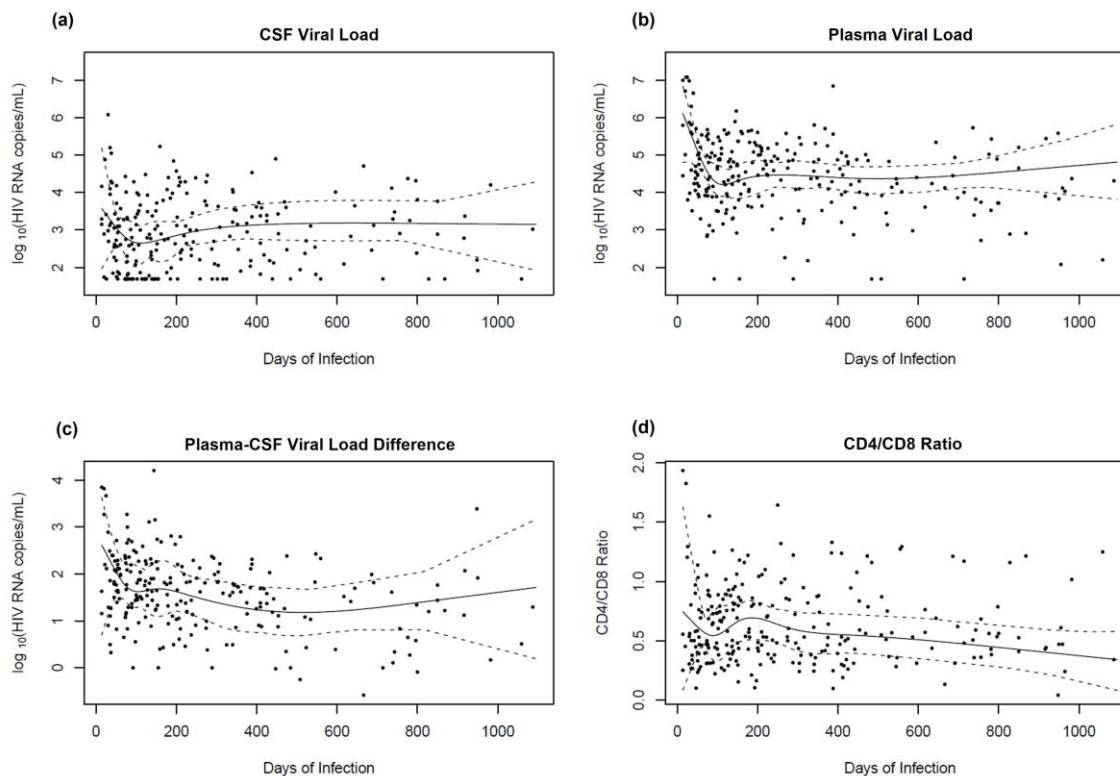


**Figure 6. Nonparametric models of (a) CSF HIV viral load, (b) plasma HIV viral load, (c) the difference in viral load between plasma and CSF, and (d) blood CD4/CD8 ratio over time in participants prior to antiretroviral therapy. Individual data points superimposed on all models.**

We were able to confirm our characterization of the mean trajectory of change in HIV viral load from the cubic splines approach using the parametric LME model with a random intercept for each subject, which revealed a significant declining mean trend up

to the second-degree polynomial prior to the 100-day knot and a significant increasing mean trend which levels off over time using the third-degree polynomial after the 100-day knot (**Table 3**). CD4/CD8 ratio was negatively correlated with CSF viral load, as there was a 0.69 (95% CI: -1.1, -0.31) unit decrease in  $\log_{10}$ (CSF HIV RNA) for each unit increase in the CD4/CD8 ratio ( $p = 0.0005$ ). Plasma viral load was found to be completely colinear with time and, therefore, was not a variable in the parametrized model.

Variable	Parameter	95% CI	p-value
Intercept	4.877	-	-
Month	-1.343	(-2.316, -0.3696)	0.0083
Month <sup>2</sup>	0.2418	(0.0235, 0.4602)	0.0330
Month <sub>100</sub>	-0.1880	(-0.7446, 0.3687)	0.5114
Month <sub>100</sub> <sup>2</sup>	-0.2460	(-0.4630, -0.0290)	0.0291
Month <sub>100</sub> <sup>3</sup>	$6.0 \times 10^{-5}$	( $-8.833 \times 10^{-5}$ , $2.085 \times 10^{-4}$ )	0.4313
CD4/CD8	-0.6919	(-1.070, -0.3140)	0.0005

**Table 3. Parameter estimates with 95% confidence intervals and p-values for the parametric LME model of HIV viral load in the CSF. Month = time since infection in months. Month<sub>100</sub> = time since 100 days post-infection, in months.**

## DISCUSSION

In this study, we created a longitudinal model for viral dynamics in the CSF of ART-naïve individuals during early HIV infection, and compared these findings to the known dynamics of HIV in plasma. Using a nonparametric smoothing cubic spline approach for modeling the mean trajectory, also confirmed by a parametric LME model, we described these dynamics over the first 36 months of infection. Together, these models show that HIV is consistently detected in the CSF in early years of acute infection.

According to our model, viral copies of HIV are present in the CSF early in the course of infection. In fact, in these cohorts, HIV RNA was measured as early as the 14<sup>th</sup> day of infection, which is the earliest detectable date in the STARHS algorithm. Other studies have shown that HIV is present in the plasma and semen early during infection and modeled the viral load over time [36, 38, 39], but such longitudinal natural history models do not yet exist for the CSF. Djomand et al. analyzed plasma in a group of 39 high-risk men in Rio de Janeiro, Brazil who were identified in early infection; however, only 21 participants in the cohort had viral loads measured within 6 months of estimated seroconversion. As the study estimated date of seroconversion based on repeated testing every 6 months with individuals who were initially seronegative, it was impossible to obtain viral loads as early during infection as we have presented. However, reassuringly, they did note a steep decline in CD4 count approximately 200 days post-seroconversion, which is reflected in our model of CD4/CD8 ratio [36].

Our choice to place a 100-day knot in the parametric LME model is supported by previous findings. Stekler et al., who studied longitudinal seminal and plasma viral loads in 89 men in Seattle, USA who were ART-naïve at the time of initial specimen collection, noted that while there was insufficient data to estimate the exact day at which a viral set point was established, sensitivity analysis determined it occurred by day 100 [39].

In contrast, Pilcher et al. analyzed plasma and semen in a cohort of 16 men in Lilongwe, Malawi with acute HIV infection, estimating that peak viral load occurs at approximately 17 days post-seroconversion in the plasma and at 30 days post-seroconversion in the semen, with a nadir by day 61 in plasma and day 68 in semen. These plasma findings contrast somewhat with our model; however, it appears their models were overparametrized given their sample size, and also featured 2 knots (at days 18 and 60.66 for plasma) [38]. This likely explains the discrepancies with our current findings. It is unclear how these knots were chosen, but our data and that of others, as previously discussed, support a single knot at 100 days.

Following seroconversion, our model shows a steep decline in CSF viral load in the first 100 days of infection, after which viral load slowly increases. In comparison with the established model for viral dynamics in the plasma, our CSF model follows the same general trajectory but at lower absolute levels of viral load [69]. Our findings support and clarify the timing of the early spread of HIV to the CNS, where the virus has been shown to cause CNS immune activation during primary infection [44] and later undergoes

replication independent of that occurring in plasma [70, 71]. This further contextualizes the neurological symptoms sometimes seen during primary HIV infection.

We found that blood CD4/CD8 ratio is significantly negatively associated with HIV viral load throughout the first 3 years of natural infection. This complements prior results from a study of the RV254/SEARCH010 cohort, where the authors found an independent correlation between CD4/CD8 ratio and CSF HIV RNA during acute infection in individuals prior to initiation of ART [72]. Moreover, a declining CD4/CD8 ratio has been found to be associated with neurocognitive deterioration independent from viral replication [73]. Even in individuals without HIV, a low CD4/CD8 ratio is a marker of the ‘immune risk phenotype,’ which itself is associated with increased morbidity and mortality [74]. Thus it is understandable that our model showed a long-term decline in the CD4/CD8 ratio in ART-naïve participants.

A major strength of this study is the prospective follow-up of participants identified early after seroconversion. The participants underwent cognitive testing, CSF sampling, and blood draws at follow-up visits as permitted, resulting in an extensive observational dataset of CNS and systemic measures in primary HIV infection from its early stages. Longitudinal observation of ART-naïve participants was possible because data collection for most participants occurred when the standard of care was to initiate ART only at specific CD4+ T cell count thresholds (fewer than 350 CD4+ T cells/ $\mu$ L) or in the setting of opportunistic infections or other conditions attributable to HIV infection. Given current guidelines for initiating treatment immediately in all individuals with an HIV infection [75], it would be ethically impermissible to recreate such a cohort and

dataset. As a result, this dataset provides an entirely unique resource for an understanding of the natural history of early HIV infection of the CNS.

This study has a few limitations, including the decreasing number of CSF measurements available for analysis later in the course of infection, as participants either left the study or initiated ART. However, our estimation method allowed us to keep all participants in the analysis, regardless of loss to follow up. Another potential limitation is the relative lack of female participants included in the overall cohort, as the PISCES cohort is predominantly composed of men, although we do not have evidence that either gender or sexuality plays a role in HIV viral dynamics. The reason for this sex imbalance is that recruitment for the San Francisco cohort (of which 75% of our final cohort was composed) occurred at a community clinic which primarily served men who have sex with men. In contrast, recruitment for the Gothenburg cohort occurred following clinical referral to an infectious disease specialist.

As this project only studied the CSF of participants who remained ART-naïve, we must consider whether initiation of ART in select individuals could have skewed the results; e.g., it is possible that those individuals who began ART had CSF viral load trajectories that differed significantly from those who were included in the study. However, the majority of participants in the overall cohort who began ART did so of their own choosing, before they met the clinical guidelines for initiation at that time, making it less likely that the exclusion of their CSF viral loads from this study after initiation would systemically skew the remaining data.

The ICC for our parametrized model indicates that there is likely inherent variability between subjects, though it is possible that there is another variable not included in the model which may account for the total variance observed. As the trajectory of CSF viral load is quite similar to that of plasma viral load, we examined the possibility of plasma viral load being such a contributing variable, but found the plasma viral load to be fully colinear with time in our model. This means that, for the parametrized model, time since infection and plasma viral load are equally important in determining the CSF viral load; as such, plasma viral load was not included as a parameter.

While this analysis describes the longitudinal trajectory of CSF HIV viral load, it cannot help us conclude whether the presence of HIV in the CSF is due to continued trafficking of HIV across the BBB versus sustained HIV replication within the CSF after initial viral translocation. Recent research has shown evidence of HIV replication in CD4+ T cells within the CSF during acute infection, suggesting that the viral load seen in the CSF originates from these T cells and not from a translocation of free virus across the BBB [76]. Findings such as these are important to contextualize our results, as they shed light on the mechanism behind establishment of this viral reservoir.

As previously mentioned, the PISCES cohort has been used in other studies to investigate CNS inflammation during primary HIV infection. Young et al. found increases in choline/creatine-containing metabolites in frontal white matter and increases in myo-inositol/creatine in parietal gray matter during the first year of infection, which attenuated (but did not reverse) following ART initiation, indicating ongoing

inflammation and gliosis in those areas which is likely irreversible even on adequate treatment. They also noted elevated baseline glutamate/creatine in the basal ganglia, with a subsequent decrease following ART initiation, indicating that the glutamate toxicity caused by HIV can potentially be reversed with prompt therapy [77].

In a separate analysis of the same cohort used in this project (participants from San Francisco, USA and Gothenburg, Sweden), Suh et al. reported progressive increases in CSF neopterin and activated CD4<sup>+</sup> and CD8<sup>+</sup> T cells, which indicate increasing CNS inflammation during primary HIV infection in ART-naïve individuals [22]. Peluso et al., in a study involving this cohort in addition to participants from Sydney, Australia and Milan, Italy, found elevated neurofilament light chain and decreased MRS metabolites when compared with controls, indicating neuronal injury during primary HIV infection [19].

Another earlier analysis using the same cohorts found that during early HIV infection (at a median of 77 days post-transmission), individuals had CSF viral loads, white blood cell counts, and neopterin and CXCL10 chemokine levels similar to those seen during chronic HIV infection [44]. Thus, our results add to the growing body of evidence – from studies of this cohort and others – that HIV enters the CNS early in infection and persists there longitudinally, and thus may contribute to further neuropathogenesis. The continued presence of HIV in the CNS results in the establishment of a reservoir for HIV, as well as neurological injury, cognitive and mood impairment, thus making a more complete understanding of this reservoir crucial for future efforts at a complete cure.

Further areas of study could include using other variables as covariates, such as neurocognitive function, CSF inflammatory markers, or CNS metabolites. Additionally, modeling CSF viral dynamics following initiation of ART could help better inform the process behind CSF escape.

## REFERENCES

1. Deeks, S.G., et al., *HIV infection*. Nat Rev Dis Primers, 2015. **1**: p. 15035.
2. Gottlieb, M.S., et al., *Pneumocystis carinii pneumonia and mucosal candidiasis in previously healthy homosexual men: evidence of a new acquired cellular immunodeficiency*. N Engl J Med, 1981. **305**(24): p. 1425-31.
3. Barre-Sinoussi, F., et al., *Isolation of a T-lymphotropic retrovirus from a patient at risk for acquired immune deficiency syndrome (AIDS)*. Science, 1983. **220**(4599): p. 868-71.
4. Gallo, R.C., et al., *Isolation of human T-cell leukemia virus in acquired immune deficiency syndrome (AIDS)*. Science, 1983. **220**(4599): p. 865-7.
5. Insight Start Study Group, et al., *Initiation of Antiretroviral Therapy in Early Asymptomatic HIV Infection*. N Engl J Med, 2015. **373**(9): p. 795-807.
6. World Health Organization, *Treat all people living with HIV, offer antiretrovirals as additional prevention choice for people at "substantial" risk*. 2015.
7. Haase, A.T., *Perils at mucosal front lines for HIV and SIV and their hosts*. Nat Rev Immunol, 2005. **5**(10): p. 783-92.
8. Finzi, D., et al., *Latent infection of CD4+ T cells provides a mechanism for lifelong persistence of HIV-1, even in patients on effective combination therapy*. Nat Med, 1999. **5**(5): p. 512-7.
9. Moir, S., T.W. Chun, and A.S. Fauci, *Pathogenic mechanisms of HIV disease*. Annu Rev Pathol, 2011. **6**: p. 223-48.
10. Giorgi, J.V., et al., *Predictive value of immunologic and virologic markers after long or short duration of HIV-1 infection*. J Acquir Immune Defic Syndr, 2002. **29**(4): p. 346-55.
11. Deeks, S.G., et al., *Immune activation set point during early HIV infection predicts subsequent CD4+ T-cell changes independent of viral load*. Blood, 2004. **104**(4): p. 942-7.
12. Giorgi, E.E., *A mathematical growth model of the viral population in early HIV-1 infections*. 2011, University of Massachusetts Amherst: Ann Arbor. p. 88.
13. Kelley, C.F., J.D. Barbour, and F.M. Hecht, *The relation between symptoms, viral load, and viral load set point in primary HIV infection*. J Acquir Immune Defic Syndr, 2007. **45**(4): p. 445-8.
14. Mellors, J.W., et al., *Prognosis in HIV-1 infection predicted by the quantity of virus in plasma*. Science, 1996. **272**(5265): p. 1167-70.
15. Deeks, S.G. and B.D. Walker, *Human immunodeficiency virus controllers: mechanisms of durable virus control in the absence of antiretroviral therapy*. Immunity, 2007. **27**(3): p. 406-16.
16. Woldemeskel, B.A., A.K. Kwaa, and J.N. Blankson, *Viral reservoirs in elite controllers of HIV-1 infection: Implications for HIV cure strategies*. EBioMedicine, 2020. **62**: p. 103118.
17. Grant, I., et al., *Evidence for early central nervous system involvement in the acquired immunodeficiency syndrome (AIDS) and other human immunodeficiency virus (HIV) infections. Studies with neuropsychologic testing and magnetic resonance imaging*. Ann Intern Med, 1987. **107**(6): p. 828-36.
18. Heaton, R.K., et al., *The impact of HIV-associated neuropsychological impairment on everyday functioning*. J Int Neuropsychol Soc, 2004. **10**(3): p. 317-31.
19. Peluso, M.J., et al., *Cerebrospinal fluid and neuroimaging biomarker abnormalities suggest early neurological injury in a subset of individuals during primary HIV infection*. J Infect Dis, 2013. **207**(11): p. 1703-12.
20. Samboju, V., et al., *Structural and functional brain imaging in acute HIV*. Neuroimage Clin, 2018. **20**: p. 327-335.

21. Sanford, R., et al., *Longitudinal Trajectories of Brain Volume and Cortical Thickness in Treated and Untreated Primary Human Immunodeficiency Virus Infection*. Clin Infect Dis, 2018. **67**(11): p. 1697-1704.
22. Suh, J., et al., *Progressive increase in central nervous system immune activation in untreated primary HIV-1 infection*. J Neuroinflammation, 2014. **11**: p. 199.
23. Wright, P.W., et al., *Putamen volume and its clinical and neurological correlates in primary HIV infection*. AIDS, 2016. **30**(11): p. 1789-94.
24. Saylor, D., et al., *HIV-associated neurocognitive disorder--pathogenesis and prospects for treatment*. Nat Rev Neurol, 2016. **12**(4): p. 234-48.
25. González, R.G., et al., *New insights into the neuroimmunity of SIV infection by magnetic resonance spectroscopy*. J Neuroimmune Pharmacol, 2006. **1**(2): p. 152-9.
26. Rahimy, E., et al., *Blood-Brain Barrier Disruption Is Initiated During Primary HIV Infection and Not Rapidly Altered by Antiretroviral Therapy*. J Infect Dis, 2017. **215**(7): p. 1132-1140.
27. Fois, A.F. and B.J. Brew, *The Potential of the CNS as a Reservoir for HIV-1 Infection: Implications for HIV Eradication*. Current HIV/AIDS Reports, 2015. **12**(2): p. 299-303.
28. Winston, A., et al., *Defining cerebrospinal fluid HIV RNA escape: editorial review AIDS*. AIDS, 2019. **33 Suppl 2**: p. S107-S111.
29. Canestri, A., et al., *Discordance between cerebral spinal fluid and plasma HIV replication in patients with neurological symptoms who are receiving suppressive antiretroviral therapy*. Clin Infect Dis, 2010. **50**(5): p. 773-8.
30. Edén, A., et al., *HIV-1 viral escape in cerebrospinal fluid of subjects on suppressive antiretroviral treatment*. J Infect Dis, 2010. **202**(12): p. 1819-25.
31. Peluso, M.J., et al., *Cerebrospinal fluid HIV escape associated with progressive neurologic dysfunction in patients on antiretroviral therapy with well controlled plasma viral load*. AIDS, 2012. **26**(14): p. 1765-74.
32. Wallet, C., et al., *Microglial Cells: The Main HIV-1 Reservoir in the Brain*. Front Cell Infect Microbiol, 2019. **9**: p. 362.
33. Spudich, S.S., *Immune activation in the central nervous system throughout the course of HIV infection*. Curr Opin HIV AIDS, 2016. **11**(2): p. 226-33.
34. Al-Harti, L., J. Joseph, and A. Nath, *Astrocytes as an HIV CNS reservoir: highlights and reflections of an NIMH-sponsored symposium*. J Neurovirol, 2018. **24**(6): p. 665-669.
35. Ko, A., et al., *Macrophages but not Astrocytes Harbor HIV DNA in the Brains of HIV-1-Infected Aviremic Individuals on Suppressing Antiretroviral Therapy*. J Neuroimmune Pharmacol, 2019. **14**(1): p. 110-119.
36. Djomand, G., et al., *Viral load and CD4 count dynamics after HIV-1 seroconversion in homosexual and bisexual men in Rio de Janeiro, Brazil*. J Acquir Immune Defic Syndr, 2006. **43**(4): p. 401-4.
37. Blackard, J.T., *HIV compartmentalization: a review on a clinically important phenomenon*. Curr HIV Res, 2012. **10**(2): p. 133-42.
38. Pilcher, C.D., et al., *Amplified transmission of HIV-1: comparison of HIV-1 concentrations in semen and blood during acute and chronic infection*. AIDS, 2007. **21**(13): p. 1723-30.
39. Stekler, J., et al., *HIV dynamics in seminal plasma during primary HIV infection*. AIDS Res Hum Retroviruses, 2008. **24**(10): p. 1269-74.
40. Power, C., et al., *Demented and nondemented patients with AIDS differ in brain-derived human immunodeficiency virus type 1 envelope sequences*. J Virol, 1994. **68**(7): p. 4643-49.
41. Pillai, S.K., et al., *Genetic attributes of cerebrospinal fluid-derived HIV-1 env*. Brain, 2006. **129**(Pt 7): p. 1872-83.

42. Harrington, P.R., et al., *Cross-sectional characterization of HIV-1 env compartmentalization in cerebrospinal fluid over the full disease course*. AIDS, 2009. **23**(8): p. 907-15.
43. Valcour, V., et al., *Central nervous system viral invasion and inflammation during acute HIV infection*. J Infect Dis, 2012. **206**(2): p. 275-82.
44. Spudich, S., et al., *Central nervous system immune activation characterizes primary human immunodeficiency virus 1 infection even in participants with minimal cerebrospinal fluid viral burden*. J Infect Dis, 2011. **204**(5): p. 753-60.
45. Gold, J.A., et al., *Longitudinal characterization of depression and mood states beginning in primary HIV infection*. AIDS Behav, 2014. **18**(6): p. 1124-32.
46. Jiang, M., et al., *Early events during BK virus entry and disassembly*. J Virol, 2009. **83**(3): p. 1350-8.
47. Hetta, H.F., et al., *Extra-hepatic infection of hepatitis C virus in the colon tissue and its relationship with hepatitis C virus pathogenesis*. J Med Microbiol, 2016. **65**(8): p. 703-712.
48. Ariede, J.R., et al., *Platelets can be a biological compartment for the Hepatitis C Virus*. Braz J Microbiol, 2015. **46**(2): p. 627-9.
49. Gheit, T., *Mucosal and Cutaneous Human Papillomavirus Infections and Cancer Biology*. Front Oncol, 2019. **9**: p. 355.
50. Van Loy, T., et al., *JC virus quasispecies analysis reveals a complex viral population underlying progressive multifocal leukoencephalopathy and supports viral dissemination via the hematogenous route*. J Virol, 2015. **89**(2): p. 1340-7.
51. Yasuda, Y., et al., *Comparison of PCR-amplified JC virus control region sequences from multiple brain regions in PML*. Neurology, 2003. **61**(11): p. 1617-9.
52. Spudich, S.S., et al., *Cerebrospinal fluid HIV infection and pleocytosis: relation to systemic infection and antiretroviral treatment*. BMC Infect Dis, 2005. **5**: p. 98.
53. Zetola, N.M. and C.D. Pilcher, *Diagnosis and management of acute HIV infection*. Infect Dis Clin North Am, 2007. **21**(1): p. 19-48, vii.
54. Janssen, R.S., et al., *New testing strategy to detect early HIV-1 infection for use in incidence estimates and for clinical and prevention purposes*. JAMA, 1998. **280**(1): p. 42-8.
55. Lindback, S., et al., *Diagnosis of primary HIV-1 infection and duration of follow-up after HIV exposure*. Karolinska Institute Primary HIV Infection Study Group. AIDS, 2000. **14**(15): p. 2333-9.
56. Price, R.W. and S.G. Deeks, *Antiretroviral drug treatment interruption in human immunodeficiency virus-infected adults: Clinical and pathogenetic implications for the central nervous system*. J Neurovirol, 2004. **10** Suppl 1: p. 44-51.
57. Price, R.W., et al., *Cerebrospinal fluid response to structured treatment interruption after virological failure*. AIDS, 2001. **15**(10): p. 1251-9.
58. Gisslén, M., et al., *Cerebrospinal fluid signs of neuronal damage after antiretroviral treatment interruption in HIV-1 infection*. AIDS Res Ther, 2005. **2**: p. 6.
59. Croxford, R., *Restricted Cubic Spline Regression: A Brief Introduction*, in SAS Global Forum. 2016: Las Vegas, Nevada.
60. Diggle, P.J. and A.P. Verbyla, *Nonparametric Estimation of Covariance Structure in Longitudinal Data*. Biometrics, 1998. **54**(2).
61. Efron, B. and R.J. Tibshirani, *An Introduction to the Bootstrap*. 1993, New York, NY: Chapman & Hall.
62. Gauthier, J., Q.V. Wu, and T.A. Gooley, *Cubic splines to model relationships between continuous variables and outcomes: a guide for clinicians*. Bone Marrow Transplant, 2020. **55**(4): p. 675-680.

63. Li, Y. and Y.G. Wang, *Smooth bootstrap methods for analysis of longitudinal data*. Stat Med, 2008. **27**(7): p. 937-53.
64. Tibshirani, R. and K. Knight, *Model Search by Bootstrap "Bumping"*. Journal of Computational and Graphical Statistics, 1999. **8**(4).
65. R Development Core Team, *R: A language and environment for statistical computing*. 2021, R Foundation for Statistical Computing: Vienna, Austria.
66. Frank E Harrell Jr with contributions from Charles Dupont and many others, *Hmisc: Harrell Miscellaneous*. 2021.
67. Little, R.J.A. and D.B. Rubin, *Statistical Analysis with Missing Data*. 2nd ed. 2002, Hoboken, NJ: John Wiley & Sons, Inc.
68. Pinheiro, J., et al., *nlme: Linear and Nonlinear Mixed Effects Models*. 2021.
69. Hill, A.L., et al., *Insight into treatment of HIV infection from viral dynamics models*. Immunol Rev, 2018. **285**(1): p. 9-25.
70. Valcour, V., et al., *Pathogenesis of HIV in the central nervous system*. Curr HIV/AIDS Rep, 2011. **8**(1): p. 54-61.
71. Sturdevant, C.B., et al., *Compartmentalized replication of R5 T cell-tropic HIV-1 in the central nervous system early in the course of infection*. PLoS Pathog, 2015. **11**(3): p. e1004720.
72. Chan, P., et al., *Distribution of Human Immunodeficiency Virus (HIV) Ribonucleic Acid in Cerebrospinal Fluid and Blood Is Linked to CD4/CD8 Ratio During Acute HIV*. J Infect Dis, 2018. **218**(6): p. 937-945.
73. Vassallo, M., et al., *A decreasing CD4/CD8 ratio over time and lower CSF-penetrating antiretroviral regimens are associated with a higher risk of neurocognitive deterioration, independently of viral replication*. J Neurovirol, 2017. **23**(2): p. 216-225.
74. Tsoukas, C., *Immunosenescence and aging in HIV*. Curr Opin HIV AIDS, 2014. **9**(4): p. 398-404.
75. Phanuphak, N. and R.M. Gulick, *HIV treatment and prevention 2019: current standards of care*. Curr Opin HIV AIDS, 2020. **15**(1): p. 4-12.
76. Sharma, V., et al., *Cerebrospinal fluid CD4+ T cell infection in humans and macaques during acute HIV-1 and SHIV infection*. PLOS Pathogens, 2021. **17**(12).
77. Young, A.C., et al., *Cerebral metabolite changes prior to and after antiretroviral therapy in primary HIV infection*. Neurology, 2014. **83**(18): p. 1592-600.